CHIN. PHYS. LETT. Vol. 38, No. 4 (2021) 043301

Strong-Field-Induced N_2^+ Air Lasing in Nitrogen Glow Discharge Plasma

Nana Dong(董娜娜)[1†], Yan Zhou(周燕)[1†], Shanbiao Pang(庞山彪)[1], Xiaodong Huang(黄晓东)[1], Ke Liu(刘珂)[1], Lunhua Deng(邓伦华)[1*], and Huailiang Xu(徐淮良)[1,2,3,4*]

[1]*State Key Laboratory of Precision Spectroscopy, East China Normal University, Shanghai 200062, China*
[2]*State Key Laboratory of Integrated Optoelectronics, College of Electronic Science and Engineering, Jilin University, Changchun 130012, China*
[3]*Chongqing Institute of East China Normal University, Chongqing 401120, China*
[4]*CAS Center for Excellence in Ultra-intense Laser Science, Shanghai 201800, China*

(Received 1 January 2021; accepted 26 January 2021; published online 6 April 2021)

We investigate N_2^+ air lasing at 391 nm, induced by strong laser fields in a nitrogen glow discharge plasma. We generate forward N_2^+ air lasing on the $B^2\Sigma_u^+(v'=0)$–$X^2\Sigma_g^+(v''=0)$ transition at 391 nm by irradiating an intense 35-fs, 800-nm laser in a pure nitrogen gas, finding that the 391-nm lasing quenches when the nitrogen gas is electrically discharged. In contrast, the 391-nm fluorescence measured from the side of the laser beam is strongly enhanced, demonstrating that this discharge promotes the population in the $B^2\Sigma_u^+(v'=0)$ state. By comparing the lasing and fluorescence spectra of the nitrogen gas obtained in the discharged and laser-induced plasma, we show that the quenching of N_2^+ lasing is caused by the efficient suppression of population inversion between the $B^2\Sigma_u^+$ and $X^2\Sigma_g^+$ states of N_2^+, in which a much higher population occurs in the $X^2\Sigma_g^+$ state in the discharge plasma. Our results clarify the important role of population inversion in generating N_2^+ air lasing, and also indicate the potential for the enhancement of N_2^+ lasing via further manipulation of the population in the $X^2\Sigma_g^+$ state in the discharged medium.

DOI: 10.1088/0256-307X/38/4/043301

The ultrafast femtosecond laser has the advantage of high peak power,[1] which results in high-intensity laser fields in a gas environment, thereby inducing the excitation and ionization of gaseous atoms and molecules.[2–6] In air, it has been demonstrated that strong-field excited molecules/ions may be population-inverted, resulting in the so-called 'air lasing' phenomenon,[7–10] which has attracted considerable attention in recent years.[11–20]

Interestingly, it has recently been shown that strong-field-induced N_2^+ air lasing on the $B^2\Sigma_u^+(v'=0)$–$X^2\Sigma_g^+(v''=0)$ transition at 391 nm is effectively enhanced in a few orders of magnitude by modulating the driven laser fields.[21–23] The underlying mechanism for this process is based on a multi-state coupling model, in which the $A^2\Pi_u$ state of N_2^+ plays a key role, serving as the population reservoir.[15] In this case, photoionization prepares most of the N_2^+ ions in their $X^2\Sigma_g^+$ ground electronic state, which is subsequently transferred to the $A^2\Pi_u$ state by the rear part of the driver laser field, leading to population inversion between $B^2\Sigma_u^+(v'=0)$ and $X^2\Sigma_g^+(v''=0)$.[15] By modulating the polarization state of the rear part of the laser pulse in time to increase the efficiency of population transfer from $X^2\Sigma_g^+$ to $A^2\Pi_u$, using a polarization-gating (PG) technique, an enhancement in the N_2^+ laser of two orders of magnitude was achieved.[21] Furthermore, an almost complete depletion of the population in the $X^2\Sigma_g^+$ state in N_2^+ was realized by combining the PG time-varying polarization light field with an additional IR light. Consequently, an enhancement in the N_2^+ lasing of 5–6 orders of magnitude was obtained.[23] It is therefore anticipated that N_2^+ lasing could be greatly enhanced by modulating the driven laser fields if a greater population could be prepared in the N_2^+.

In this study, we investigate the 391-nm lasing actions of N_2^+, induced by a strong laser field in a nitrogen glow discharge plasma, capable of heating nitrogen molecules and thereby increasing the number density of ionized nitrogen molecules. We measure the strong field-induced N_2^+ lasing in both pure nitrogen gas and discharge plasma, finding that the glow discharge plasma has a negative effect on the generation of the 391 nm lasing; i.e., the 391-nm lasing undergoes significant quenching when the nitrogen gas is electrically discharged. The mechanism of the plasma's action during air lasing is demonstrated by comparing variations in the side-view fluorescence and externally seeded N_2^+ lasing, both in pure nitrogen gas, and in

Supported in part by the National Natural Science Foundation of China (Grant Nos. 61625501 and 62027822), and the Open Fund of the State Key Laboratory of High Field Laser Physics (SIOM).
†These authors contributed equally to this work.
*Corresponding authors. Email: lhdeng@phy.ecnu.edu.cn; huailiang@jlu.edu.cn
© 2021 Chinese Physical Society and IOP Publishing Ltd

nitrogen glow discharge plasma. This highlights the key role of population inversion in the generation of N_2^+ lasing.

The experiments were conducted using a Ti:sapphire chirped-pulse amplification laser system (Coherent Inc. Astrella), which produced 35 fs laser pulses centering at 808 nm, with a maximal pulse energy of 7 mJ, and a repetition rate of 1 kHz. The experimental setup and optical arrangement are shown in Fig. 1. The 7 mJ laser pulse was first attenuated to 3 mJ, before being split into two parts by a beam splitter with an energy ratio of 5 : 5. One part was frequency-doubled to 400 nm by a β-BaB_2O_4 (BBO) crystal, serving as an external seed. The energy of the other part was controlled using a half-wave plate and a polarizing beam splitter. By passing a dichroic mirror, the 800 nm and the 400 nm laser pulses were collinearly propagated. An optical delay line was inserted in the 800-nm laser path to adjust the temporal delay between the 400 nm and 800 nm laser pulses. The 800 nm and 400 nm beam was then focused into a gas chamber filled with a high-purity nitrogen gas, via an $f = 20$ cm fused silica lens. Copper electrodes (copper rings, with a diameter of 2 cm, and a thickness of 1 mm) were placed at both ends of the gas chamber. High voltages can be loaded through the electrodes, so as to generate discharge plasma in the gas chamber.

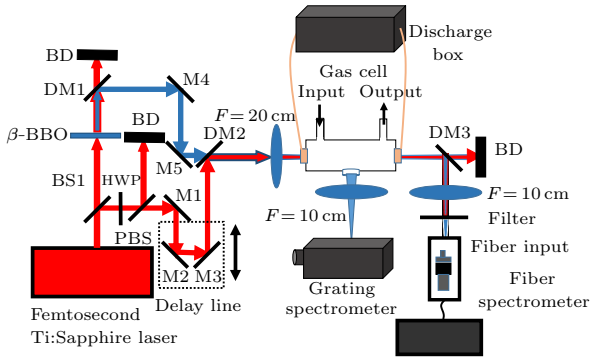

Fig. 1. Schematic diagram of the experimental apparatus for air lasing and fluorescence measurements. BS: beam splitter; M1-M5: mirrors; HWP: half-wave plate; PBS: polarizing beam splitter; BD: beam dump; DM: dichroic mirror.

The forward-propagating lasing emission generated at 391 nm was collected by a fiber connected to a grating spectrometer (HR4000+, Ocean Optics), whereas the residual pump laser was removed using a stack of bandpass filters. We chose a relatively low gas pressure (i.e., 14 mbar) in all measurements, so as to minimize the white-light generation produced by nonlinear propagation of the pump pulses. In addition, relatively low pressure is a more suitable environment for the generation of glow discharge, i.e., the selected low gas pressure is favorable for glow discharge generation, as well as for measurements of discharged- and laser-induced emissions in the visible and near-infrared range. A grating spectrometer (Princeton Instruments Acton SP2750) captured the side-view fluorescence and the discharge plasma emission.

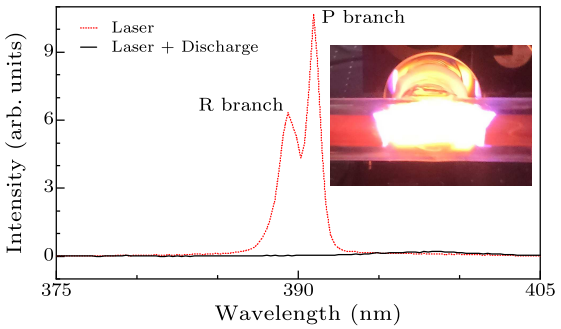

Fig. 2. Spectra of N_2^+ lasing obtained with (Laser + Discharge) and without (Laser) glow discharge. Inset: image of N_2 gas discharge, captured using a digital camera.

Figure 2 shows the self-seeded forward 391-nm lasing spectra induced by the strong laser field in pure nitrogen gas, both with and without the glow discharge induced by our home-made discharge device. The laser's incident power was set at 1.2 mJ/pulse, and the laser-induced plasma spark was located between the two copper ring-electrodes, separated by a distance of 2 cm. A vacuum pump was used to provide the cell with a continuous nitrogen supply, and the nitrogen pressure flow in the cell was maintained at a stable value of 14 mbar. The discharge voltage was set at 1.88 kV, and the spacing between the two electrodes was 2 cm. The inset of Fig. 2 shows an image of the N_2 glow discharge, captured by a digital camera. It is evident in Fig. 2 that in the scenario without glow discharge (dotted red line), two strong peaks appear at about 391 nm, which are assigned to the R and P branches of the $B^2\Sigma_u^+(v' = 0)$–$X^2\Sigma_g^+(v'' = 0)$ transition of N_2^+. However, when the gas is electronically discharged (black solid line), the N_2^+ lasing peaks disappear completely, demonstrating that discharge plasma exercises a negative effect on the generation of N_2^+ lasing. This result is totally different from our expectations, in that we anticipated that glow discharge would result in an enhancement of N_2^+ lasing, since the glow discharge would heat the nitrogen gas and generate high concentration N_2^+ ions.

To explore the underlying mechanism responsible for the quenching of the 391 nm lasing induced by the glow discharge, we measured the emission spectra of the plasma induced respectively by the laser (green solid line), discharge (red dashed line) and both of them (referred as laser + discharge) (black dotted line). The results are shown in Fig. 3. The emission spectra were recorded from the side of the discharge cell, where the optical arrangement is as shown in

Fig. 1. For clarity, Fig. 3(b) shows an enlargement of the laser-induced fluorescence spectrum given in Fig. 3(a). Figure 3 clearly shows that the three spectra at around 391 nm have similar spectral structures, but that the intensity of the signals induced by the laser alone is much weaker than signals induced via discharge, or by laser + discharge. The spectral intensity is at its strongest when the discharge and the laser coexist.

In the case for the laser alone, the laser field ionizes the N_2 and prepares the population in the $B^2\Sigma_u^+$ state of N_2^+, resulting in the 391-nm emission; the $X^2\Sigma_g^+$ state is populated, but with a smaller population than the $B^2\Sigma_u^+$ state, due to post-ionization optical coupling,[15] leading to population inversion and 391-nm lasing. Similarly, in the discharge case, the $B^2\Sigma_u^+$ state of N_2^+ has a considerable population in the glow discharge plasma, resulting in a much stronger spectral intensity than that achieved via laser-induced emission. In particular, with discharge plasma, the population of N_2^+ lying in different states may exhibit Boltzmann distribution, so that the population of the $X^2\Sigma_g^+$ state may be very high, far larger than that of the $B^2\Sigma_u^+$ state. As a result, in the laser + discharge case, although the population in the $B^2\Sigma_u^+$ state increases, that of the $X^2\Sigma_g^+$ state will increase more, making it difficult to achieve population inversion between the $B^2\Sigma_u^+$ state and $X^2\Sigma_g^+$ state, resulting in the disappearance of the 391-nm lasing. Interestingly, the signal intensity of the laser + discharge case is greater than the sum of the spectral intensity of the other two cases, indicating that discharge favors photoionization, and to the generation of increased numbers of N_2^+ ions.

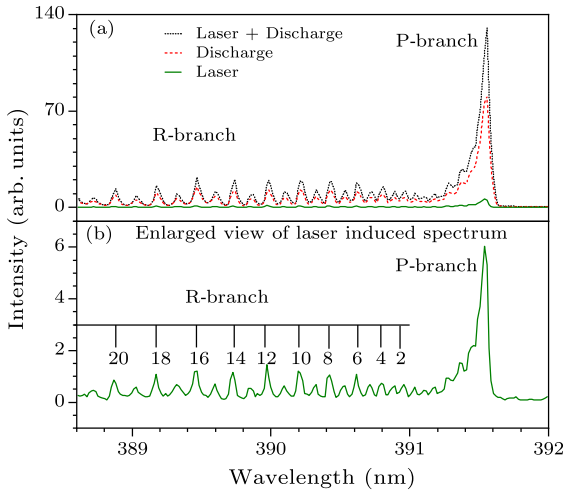

Fig. 3. (a) Side-view spectra of the laser-induced fluorescence spectrum, the plasma emission spectrum, and the spectrum of combined discharge and filament. (b) Enlarged view of the laser-induced fluorescence spectrum.

Another possible reason for the disappearance of air lasing in discharge plasma may be the variation in the self-seeded light at about 400 nm, due to the production of discharge plasma. To clarify the reason behind the disappearance of the 391 nm lasing, we reduced the incident power of the 800-nm pump laser's 0.5 mJ/pulse so that no self-seeded lasing can be observed. We then introduced a 400-nm laser as the external seed to produce the N_2^+ lasing pulse, as indicated by the red dotted line in Fig. 4. The gas pressure remains at 14 mbar. Similarly to Fig. 2, when the nitrogen gas is electrically discharged, the spectral peak at 391 nm disappears, demonstrating the minor role of the self-seed in the reduction of N_2^+ lasing, and that the discharge changes the condition of the population inversion between the $B^2\Sigma_u^+$ and $X^2\Sigma_g^+$ states for N_2^+ lasing at 391 nm.

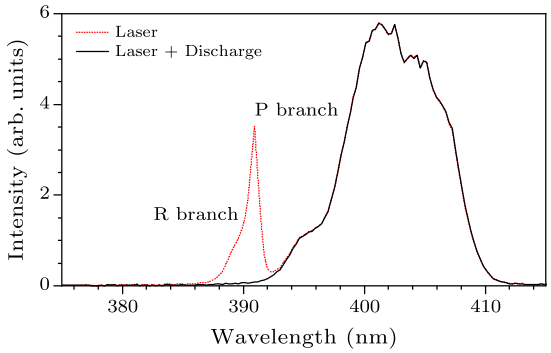

Fig. 4. Spectra of 391 nm lasing, observed with (Laser + Discharge) and without (Laser) glow discharge under an external seed.

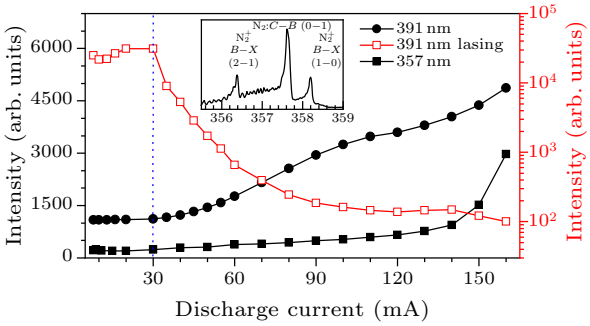

Fig. 5. Spectral intensities of laser-induced lasing at 391 nm, and fluorescence at 391 nm and 357 nm as a function of discharge current. Inset: fluorescence spectrum of N_2 at around 357 nm.

To further investigate the discharge effect, we changed the excitation and ionization rates of the nitrogen molecules by adjusting the discharge current. Figure 5 shows that the 391-nm lasing intensity (open rectangle) varies as the discharge current increases. For comparison, we also recorded the intensities of N_2 fluorescence at 357 nm (solid rectangle), and N_2^+ fluorescence at 391 nm (solid circle) as a function of the discharge current, where the 357 nm peak corresponds to the (0–1) band of the $C^3\Pi_u \rightarrow B^3\Pi_g$ transition

system of N_2, as shown in the inset panel. As shown in Fig. 5, the 391-nm lasing and the fluorescence at both 357 nm and 391 nm remain constant when the current is smaller than 30 mA, below which no discharge occurs. As the current further increases, i.e., the discharge takes place and becomes stronger, lasing decreases rapidly, but fluorescence increases. This means that the populations in both the $C^3\Pi_u$ state of N_2 and the $B^2\Sigma_u^+$ state of N_2^+ increase at the higher discharge current region, but the decease in lasing intensity in the higher current region means that the glow discharge plasma results in a greater N_2^+ population for the $X^2\Sigma_g^+$ state, reducing the population difference between the $B^2\Sigma_u^+$ and $X^2\Sigma_g^+$ states. Finally, the $B^2\Sigma_u^+$ state's population is equal to, or below that of the $X^2\Sigma_g^+$ state, which destroys the population inversion required for air lasing.

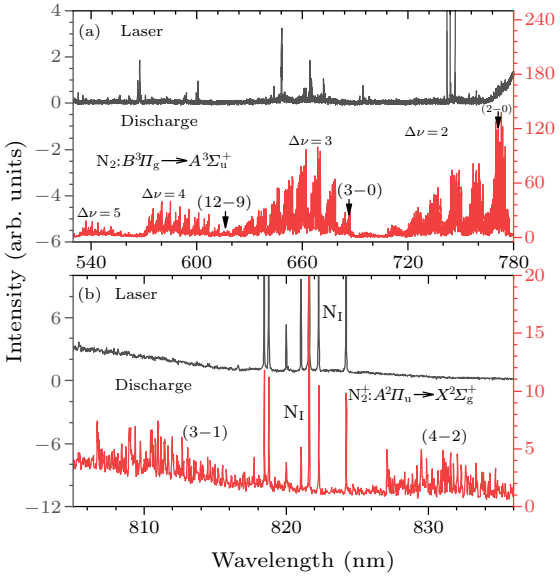

Fig. 6. Comparison of the spectra of N_2 induced by laser and discharge. (a) Part of the $B^3\Pi_g \rightarrow A^3\Sigma_u^+$ spectrum of N_2. (b) Part of the $A^2\Pi_u \rightarrow X^2\Sigma_g^+$ spectrum of N_2^+.

In order to carefully examine the possible influence of discharge on the population distribution in the N_2^+ ions induced by a strong laser field, we further compare the laser-induced emission spectra of N_2 and N_2^+ with those obtained for glow discharge. As shown in the inset of Figs. 5 and 6(a), all three excited states, $C^3\Pi_u$, $B^3\Pi_g$, and $A^3\Sigma_u^+$, are involved in the discharge-induced spectrum of N_2, where the spectral intensity of the $B^3\Pi_g \rightarrow A^3\Sigma_u^+$ system is extremely strong, such that even the optical emissions of certain high vibrational levels of the $B^3\Pi_g$ state, such as the $v = 12$ vibrational level, i.e., the (12–9) band, can be clearly observed, as labeled in the figure. However, in the laser-induced spectrum [see Fig. 6(a)], the spectral bands coming from the $B^3\Pi_g \rightarrow A^3\Sigma_u^+$ system cannot be observed at all. On the other hand, as shown in Figs. 3 and 6(b), the two excited states, $B^2\Sigma_u^+$ and $A^2\Pi_u$, are involved in the discharge emission spectrum of N_2^+, where the $A^2\Pi_u \rightarrow X^2\Sigma_g^+$ transition, located at around 820 nm, is clearly observed [see Fig. 6(b)]; however, in the laser-induced spectrum, the fluorescence emission on the $A^2\Pi_u \rightarrow X^2\Sigma_g^+$ transition is unobservable. This means that the populations in the $B^3\Pi_g$ state of N_2 and the $A^2\Pi_u$ state of N_2^+ in the laser-induced plasma are not as high as those in the discharge plasma. In other words, when the discharge is induced, the population in N_2^+ is dominated by the Boltzmann distribution, which has long been an area of interest in the field of absorption spectroscopy.[24,25] This indicates that the laser-induced populations in the $A^2\Pi_u$, $B^2\Sigma_u^+$, and $X^2\Sigma_g^+$ states of N_2^+ are far from Boltzmann distribution, so that it is possible to generate the population inversion required for air lasing. As a consequence, the negative effects of the discharge on the N_2^+ lasing are the result of an increased population in the ground $X^2\Sigma_g^+$ state of N_2^+ induced by the discharge, which ruins the laser-induced population inversion between the $B^2\Sigma_u^+$ and $X^2\Sigma_g^+$ states, resulting in a reduction in 391-nm lasing.

In summary, we have investigated the glow discharge effect on the generation of N_2^+ lasing in a strong femtosecond laser field, and demonstrated experimentally that the intensity of the $B^2\Sigma_u^+(v = 0)$ and $X^2\Sigma_g^+(v = 0)$ lasing lines of N_2^+ at 391 nm are strongly reduced by discharged plasma. We have identified the mechanism of the significant decrease in N_2^+ lasing intensity by comparing the lasing and fluorescence spectra of nitrogen molecules in both discharged and laser-induced plasma, and found that the discharge induces a much larger population in the ground $X^2\Sigma_g^+$ state than in the $B^2\Sigma_u^+$ state of N_2^+, leading to an effective suppression of the population inversion between the $B^2\Sigma_u^+$ and $X^2\Sigma_g^+$ states of N_2^+. Our results not only clarify the key role of population inversion in generating N_2^+ air lasing, but also provide a way to enhance the population in the ground $X^2\Sigma_g^+$ state of N_2^+, which can be transferred to the $A^2\Pi_u$ state by manipulating intense laser fields for the further enhancement of N_2^+ lasing.[22]

References

[1] Li R X, Leng Y X and Xu Z Z 2015 *Physics* **44** 509
[2] Xu H L, Cheng Y, Chin S L and Sun H B 2015 *Laser & Photon. Rev.* **9** 275
[3] Wei X Y, Tu Z W, Liu C, Li H L and Xu H L 2016 *Chin. Phys. Lett.* **33** 054201
[4] Chin S L and Xu H L 2016 *J. Phys. B* **49** 222003
[5] Yuan J, Ma Y, Li R, Ma H, Zhang Y, Ye D, Shen Z, Yan T, Wang X, Weidemuller M and Jiang Y 2020 *Chin. Phys. Lett.* **37** 053201
[6] Sun T, Zhang S W, Wang R, Feng S, Liu Y, Lv H and Xu H F 2020 *Chin. Phys. Lett.* **37** 043301
[7] Luo Q, Liu W and Chin S L 2003 *Appl. Phys. B* **76** 337
[8] Yao J P, Zeng B, Xu H L, Li G H, Chu W, Ni J L, Zhang

H S, Chin S L, Cheng Y and Xu Z Z 2011 *Phys. Rev. A* **84** 051802
[9] Dogariu A, Michael J B, Scully M O and Miles R B 2011 *Science* **331** 442
[10] Li H L, Yao D W, Wang S Q, Fu Y and Xu H L 2019 *Chin. Phys. B* **28** 114204
[11] Kartashov D, Ališauskas S, Andriukaitis G, Pugžlys A, Shneider M, Zheltikov A, Chin S L and Baltuška A 2012 *Phys. Rev. A* **86** 033831
[12] Zhang H S, Jing C R, Yao J P, Li G H, Zeng B, Chu W, Ni J L, Xie H Q, Xu H L, Chin S L, Yamanouchi K R, Cheng Y and Xu Z Z 2013 *Phys. Rev. X* **3** 041009
[13] Chu W, Li H L, Ni J L, Zeng B, Yao J P, Zhang H S, Li G H, Jing C R, Xie H Q, Xu H L, Yamanouchi K R and Cheng Y 2014 *Appl. Phys. Lett.* **104** 091106
[14] Mitryukovskiy S, Liu Y, Ding P J, Houard A and Mysyrowicz A 2014 *Opt. Express* **22** 12750
[15] Xu H L, Loetstedt E, Iwasaki A and Yamanouchi K 2015 *Nat. Commun.* **6** 8347
[16] Liu Y, Ding P J, Lambert G, Houard A, Tikhonchuk V and Mysyrowicz A 2015 *Phys. Rev. Lett.* **115** 133203
[17] Yao J P, Jiang S C, Chu W, Zeng B, Wu C Y, Lu R F, Li Z T, Xie H Q, Li G H, Yu C, Wang Z S, Jiang H B, Gong Q H and Cheng Y 2016 *Phys. Rev. Lett.* **116** 143007
[18] Xu H L, Lötstedt E, Ando T, Iwasaki A and Yamanouchi K 2017 *Phys. Rev. A* **96** 041401
[19] Zhang A, Lei M W, Gao J S, Wu C Y, Gong Q H and Jiang H B 2019 *Opt. Express* **27** pp 14922
[20] Wang S Q, Fu Y, Yao D W, Chen S M, Zhang W, Li H L and Xu H L 2019 *Chin. Phys. B* **28** 123301
[21] Li H L, Hou M Y, Zang H W, Fu Y, Lötstedt E, Ando T, Iwasaki A, Yamanouchi A and Xu H L 2019 *Phys. Rev. Lett.* **122** 013202
[22] Ando T, Lötstedt E, Iwasaki A, Li H L, Fu Y, Wang S Q, Xu H L and Yamanouchi K 2019 *Phys. Rev. Lett.* **123** 203201
[23] Li H X, Lotstedt E, Li H L, Zhou Y, Dong N N, Deng L H, Lu P F, Ando T, Iwasaki A, Fu Y, Wang S Q, Wu J, Yamanouchi K and Xu H L 2020 *Phys. Rev. Lett.* **125** 053201
[24] Collet D and Huet T R 1999 *J. Mol. Spectrosc.* **197** 46
[25] Zhang Y P, Deng L H, Zhang J and Chen Y Q 2015 *Chin. J. Chem. Phys.* **28** 134